AirForce: Personal Fabrication of Large-Scale, Load-Bearing Animatronics

Structures from a Single Tube

- 3 First Author's Name, Initials, and Last name*
- 4 First author's affiliation, an Institution with a very long name, xxxx@gmail.com

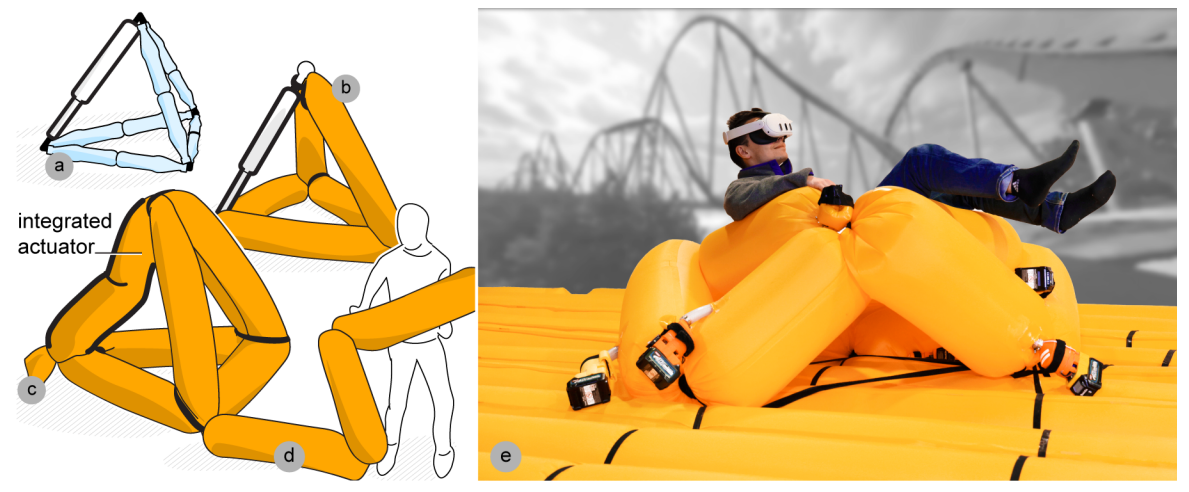


Figure 1: AirForce is a fabrication system that allows users to fabricate large-scale, load-bearing, animated structures. (a) AirForce builds on the concept of animated truss structures. (b) By replacing not only the static elements with tube, (c) but also introducing integrated tube-based actuators, AirForce allows creating entire animated structures by (d) folding up a single long tube. (e) Improved high-pressure seals and custom blowers enable structures to lift human weight, such as this 6 DoF motion platform.

We present a fabrication system called AirForce that allows users to create large-scale, load-bearing animated structures from a single tube. AirForce builds on the personal fabrication of animated truss structures, based on which it replaces not only the static elements with tube, but also introduces tube-based actuators that integrate with that same tube. This allows AirForce to create entire animated structures by folding up a single long tube. The resulting hubless single-tube design allows for efficient single-person assembly, offers an excellent power-to-weight ratio, easy transport and setup, and allows unfolding and refolding a design into a different actuated structure with 100% material reuse. We present three variants of integrated pneumatic actuators for three types of requirements: buck-ling actuators allow for long-amplitude push action; muscle actuators allow pulling, and telescoping actuators produce large forces. Combined with a lap-sealed tube design capable of holding high pressure, these actuators produce sufficient force to lift human weight. AirForce offers an end-to-end fabrication process that allows users to fabricate animated single-tube truss structures efficiently: a blender plugin allows users to model truss structures, place actuators, and route the tube so as to minimize the number of required blowers. The plugin then exports building instructions in the form of instruction labels that show where to constrict the tube, where to seal, where to insert custom inlets and blowers, and how to tie and fold the tube into the desired structure. A custom app then allows animating the resulting structures. In our technical evaluation, the three actuator types sustained a pressure of 200mBar, using which they delivered 480N, 1420N, and 2330N peak force, respectively. We demonstrate a 6DOF VR motion platform that lifts humans and an 8m high, 16m long animatronic T-Rex that animates with three degrees of freedom.

 ${\tt CCS\ CONCEPTS} \bullet {\bf Human-centered\ computing} \bullet {\tt \sim} {\bf Human\ computer\ interaction\ (HCI)} \bullet {\bf Interactive\ systems\ and\ tools}$

26 to

Additional Keywords and Phrases: truss, space frames, personal fabrication, soft robotics, inflatables.

ACM Reference Format: Anonymous for review

1 INTRODUCTION

 Researchers in architecture have demonstrated how to create human-sized to building-sized physical structures, such as bridges, roofs, and buildings, from node-and-link structures, also known as *trusses* [3]. Building on this, researchers in human-computer interaction tackled the topic using *personal* fabrication (e.g., *TrussFab* [14]). This gave non-experts the ability to create large-scale structures.

More recently, researchers further simplified the process by demonstrating the fabrication of large-scale structures from a single long piece of inflatable tube (*AirTied* [40]). Such *single-tube truss structures* offer an excellent strength-to-weight ratio and thereby allow for very large scale. Furthermore, the fact that there is only a single building element, i.e., the tube, eliminates hubs and joints and thereby greatly reduces the number of individual parts to visually search for. This vastly simplifies assembly.



Figure 2: 16m long and 8m high animatronics sculpture of a T-Rex, made from 250m tube.

In this paper, we present a fabrication system called AirForce that allows a single user to create large-scale, load-bearing single-tube truss structures capable of *actuation*. Figure 1 illustrates the core design idea: (a) Animated truss structures have historically been created from one building element per edge (e.g., *PneuMesh* [8], *Input Output Truss* [52], *TrussFormer* [13]). (b) AirForce improves on this by not only replacing the static structure with inflatable tube, (c) but also introducing integrated tube-based actuators, AirForce allows creating entire animated structures by folding up a

single long tube. (d) Improved high-pressure seals and custom blowers enable structures to lift human weight, such as this 6 DoF motion platform.

The resulting hubless single-tube design allows for efficient single-person assembly, offers an excellent power-to-weight ratio, easy transport and setup, and allows unfolding and refolding a design into a different actuated structure with 100% material reuse.

As illustrated by the 16m long 8m high animatronic T-Rex shown in Figure 2, three different variants of integrated pneumatic actuators allow handling three types of requirements: *buckling* actuators allow for long-amplitude push action, here opening and closing the dinosaur's jaw. *Muscle* actuators allow pulling, here moving the dinosaur's tail up and down, and *telescoping* actuators produce large forces, here allowing the entire 60kg structure to tilt.

2 CONTRIBUTION, BENEFITS, AND LIMITATIONS

Our main contribution is the core idea of replacing not only the static elements of a truss structure with tube, but also to introduce tube-based actuators, thereby allowing entire animated structures to be folded up from a single long tube.

As illustrated by Figure 3, the resulting hubless single-tube design offers several benefits: it allows for efficient assembly by a single person (as the structure can be assembled on the ground), allows unfolding and refolding a design into a different actuated structure with 100% material reuse, easy transport and setup, and offers an excellent power-to-weight ratio capable of lifting human weight in human-safe application.



Figure 3: (a) AirForce allows a single user to create large-scale animated structures efficiently from a single tube by (b) adding constrictions, (c) adding custom inlets and custom blowers, pre-inflating tubes, (d) tying up the truss structure, and (e) fully inflating the structure. (g) AirForce also allows unfolding and (h) refolding a structure into a different design with 100% material reuse.

Our second main contribution is a fabrication system called AirForce that supports users in creating such large-scale, load-bearing animated structures from a single tube efficiently. To maximize democratization, we are intentionally opting for a *semi*-automated process that does not require specialized equipment (*AirTied* [40]) and implement our software as a blender plug-in to leverage user familiarity with the design software.

The AirForce blender plugin allows users to model truss structures, place actuators, and route the tube so as to minimize the number of required blowers. The plugin then exports building instructions in the form of instruction labels that show where to constrict the tube, where to seal, where to insert custom inlets and blowers, and how to tie and fold the tube into the desired structure. A custom app then allows animating the resulting structures.

Limitations include: (1) The blowers are noisy, > 60dB. (2) The force profile of AirForce pneumatic actuators is not as linear as traditional pneumatic actuators. (3) Our blower app provides pressure control per blower (through integrated sensor), however, relies on the user to consider the effect on the actuators.

We will open-source the entire project, including inlet, blower, circuit designs, blender extension, control app, and the VR experience for driving the motion platform shown in Figure 1d.

Meta comment, only for review: We have done our best to anonymize this work, including the video. That said, as the CHI author's guide acknowledges, some projects are harder to anonymize than others, and this one is certainly one

of the harder ones, as it takes place in the physical world and because of its scale. We thank the reviewers for their understanding.

3 RELATED WORK

 $\begin{array}{c} 106 \\ 107 \end{array}$

This paper builds on research on actuated truss structures, large-scale soft robotics, soft pneumatic actuators, portable pressure supplies, and integrated fabrication.

3.1 Inflatable Soft Robotics

In Soft Robotics, i.e., the discipline of building actuated robots from compliant materials such as fabrics or silicone [43], many projects focus on designs that are only a few centimeters in size. However, several works demonstrated the utility of large-scale soft robotics: They afford large form factors, e.g., a 7m-long robot arm [53], enable room-scale haptics (e.g., *TilePop* [47], *LiftTiles* [50]), reach narrow spaces by 'growing' robots [44], carry weights significantly larger than the robot itself (e.g., *OtherLab Roach Ant* [37]), and allow making 20m high, kinematic structures (e.g., *Border Crossers* [25]).

3.2 Pneumatic Actuators for Soft Robotics

Researchers explored a plethora of soft actuator designs to actuate soft robots. They feature a range of different performance characteristics, such as actuation stroke, payload, speed, contraction vs. extension, air consumption, rigidity, controllability, etc. Our main consideration in designing actuators for AirForce was the ability to seamlessly integrate into a single tube structure, without introducing any additional hardware.

Pneumatic artificial muscles [16] have been widely researched and used since the 1950s. The original Pneumatic Artificial Muscle design by McKibben was a contracting actuator made from an inflatable rubber bladder and braided sleeve. It is used in industry (e.g., Festo Fluidic Muscle [6]), robotics research (e.g., McKibben Tensegrity Robots [12]), and HCI (e.g., OmniFiber [10]) for its large output force and fast reaction time.

Our *integrated muscle actuator* design is based on the *Series Pneumatic Artificial Muscle* by Greer et al. [7], shown in Figure 4a. This design is segmenting a tube into multiple bladders that contract when inflated by forcing the tube material into a longer path. While the original design was used in isolation, we integrated this into our single tube structure, where the tied nodes at the endpoints perform the role of the seals and act as connection points at the same time.



Figure 4: (a) Series Pneumatic Artificial Muscle by Greer et al. [7] (b) Unfolding Actuator by O'Neill et al. [36], and (c) Buckling Inflatable Tubes by Lee et al. [17].

A large class of pneumatic actuators focuses on producing *bending* motion. A popular approach to this is combining an extensible bladder with an inextensible, constraining elements. This has been demonstrated by the example of a silicon-cast 'spider' robot [48], robotic grippers made from silicon and yarn [4], CNC-knitted sleeves made from silicon [23], and by combining extensible fabric with inextensible plastic [32]. Brockner et al. [2] demonstrated a novice-friendly design tool for this class of actuators called *SoRoCAD*. Another way to produce bending motion is by creating pneumatic bladders with asymmetric welding patterns, e.g., *Pouch Motors* [30], Large-Scale *Pouch Motors* [35], *Aeromorph* [38], *Printflatables* [45], and *SnapInflatables* [58]. These custom bladders even afford position control, as demonstrated by Oka et al. [34] with a hinge actuator and Park et al. [39] with a full robotic arm.

However, the simplest way to create a bending moment is by using buckled inflatable beams, such as those by O'Neill et al. [36] or Lee et al. [17], shown in Figure 4 (b) (c). When applying pressure to a buckled inflatable tube, it produces torque that opposes the buckling. This results in a rotational movement around the axis of the kink, also known as the moment.

Our *integrated buckling actuator* builds on this idea of a buckling inflatable beam, with the significant difference that we integrate these buckling tubes into our single-tube design without the use of any further supporting or guiding elements.

Finally, only loosely inspired by previous work (*ConeAct* [19]), we developed a third version of an integrated pneumatic actuator for handling high loads, which we call the *integrated telescoping actuator*. Here, we utilize the spherical dome ending of a tube member as an actuation pouch, while preventing the tube itself from ever buckling by maintaining minimal pressure at all times (see section: Integrated Telescoping Actuator).

3.3 Powering Pneumatic Structures

- While pneumatic structures in HCI tend to be powered using conventional (displacement) compressors (e.g., FlowIO [49],
- 129 LiftTiles [50], OmniFiber [10]) alternative approaches to compact pneumatic pressure supplies are based on evaporation
- 130 [28], chemical reaction [56], ambient temperature fluctuations [22] for integrating pneumatic pressure supplies into
- 131 structures

116

117

118119

120121

122

123

124

125

126

127

139

146

- 133 sufficiently high pressure (>100mbar). In this paper, we therefore propose to use dynamic compressors directly to control
- actuators, more specifically, *blowers* [29].
- Our work furthermore proposes a design for a, so called, Heimlich valve that allow users to add an air inlet without
- 136 welding equipment and keeps air inside the structure when blowers are off (see Figure 12a). Beyond its original function
- of draining water from lungs, Heimlich valve designs that are commonly sealed into mylar balloons [20] and inflatable
- packaging [21]. However, these previous designs cannot be added once *after* the sealing process of the product.

3.4 Actuated Truss Structures

- 140 A truss that includes a single linear actuator tends to deform at many joints at once. This design, called a variable
- 141 geometry truss, was proposed in 1985 by Miura et al. [27], as well as Rhodes et al. [41], as a means for making large
- structures that can be folded up automatically for transport into space. While the original design does not specify a
- specific type of actuator, robotics researchers demonstrated different actuation modes, such as electric linear actuators,
- hydraulic actuators (e.g., Kurita [15]), electric telescopic actuators (e.g., Odin [24]), zipper-actuators (e.g., Spinos et al.
- [51]), and Pneumatic Artificial Muscles (e.g., Kobayashi et al. [12]).
 - In HCI, the concept gained popularity due to its flexible shape-shifting capabilities: Swaminathan et al. proposed using
- inflatable truss structures for actuation and sensing to enable interactive devices [52]. Usevitch et al. [54] proposed an
- 148 actuated truss robot made from inflatable tubes. Its nodes are comprised of motorized rollers that move forward and
- backward along the tube, which allows it to alter node locations as a means of actuation.
- To enable more users to fabricate truss structures, *TrussFormer* [13] (and *PneuMesh* [8] for small-scale structures) pro-
- posed end-to-end fabrication workflows to design, program, and 3D print general variable-geometry-truss structures.
- 152 Users start by designing the static shape first in a software tool, replacing edges with actuators, and programming the
- motion. The systems then generate the nodes for 3D printing and manual assembly.

This paper draws inspiration from these workflows, however structures in this work are hub-less, eliminating the

(non-reusable, >>100h to 3D print) custom nodes TrussFormer uses. Getting rid of this 3D printing step speeds up the

overall fabrication process by >10x.

3.5 Personal Fabrication of Large-Scale Structures

While most projects in soft robotics or actuated structures treat the structure, rather than the fabrication process, as

their main contribution, works on the fabrication process show a way forward towards allowing a wider audience to

fabricate large-scale structures.

The most common way of integrating actuators with a static structure is by using 3D printer-like fabrication devices:

Wehner et al., for example, present an integrated system for fabricating autonomous walking soft robots using a silicone

dispenser [57]. Aeromorph [38] and Printflatables [45] used a CNC heat-sealing device to selectively seal two layers of

fabric to achieve actuation. In addition to actuation, AirLogic [46] also fabricates control and computation using off-the-

shelf FDM printers.

155

157

164

167

168

170

176

177

180

184

187

188

One drawback of using a fabrication device that encloses the structure, such as a 3D printer, is that the structure

cannot surpass the size of the fabrication device. This makes this approach unsuitable for the fabrication of large-scale

structures. Instead, large-scale truss structures tend to get assembled from multiple parts (e.g., MERO system [26]) or

from a combination of 3D-printed parts and ready-made parts (e.g., TrussFab [14] and Digital Bamboo [11]).

3.6 Single tube structures

While the fabrication of large-scale structures historically involved piecing together many parts, AirTied [40] instead

172 unrolls a single inflatable tube, holds on to selected segments, and ties segments into nodes. Inflating the tube produces

the desired structure without the need for any scaffolding, which allows for the making of large structures using small

174 equipment.

AirForce builds on this line of work by introducing actuation and a process that does not rely on an assembly device,

while maintaining the single-tube nature of the design.

4 AIRFORCE'S THREE INTEGRATED ACTUATOR TYPES

As mentioned earlier, Airforce offers three types of actuators. As already shown in Figure 1a, actuators are always part

of a single-tube truss structure.

4.1 Integrated Buckling Actuator

181 Figure 2 shows the working principle of AirForce's integrated buckling actuator, here used to animate the jaw of the T-

182 Rex sculpture. As shown, inflating the integrated buckling actuator causes it to unbuckle and thereby drive its two

183 endpoints apart, which is here used to close the jaw. Releasing air pressure makes the actuator compliant, causing the

associated structure to collapse under the influence of gravity, here opening the jaws.

When inflated to 200 millibars, a 1.5m integrated buckling actuator allows lifting a 30kg load (see section: "Actuator

186 Performance"). To obtain a more linear force profile, we typically do not fully extend buckling actuators, but operate

them between different degrees of buckling. Not shown: an optional Velcro tie at the center of the actuator can be used

to prime the actuator to buckle at this specific point.

4.2 Integrated Telescoping Actuator

Figure 5 shows a close-up of the *integrated telescoping actuator* type. While this actuator resembles the buckling type, we never allow it to buckle. We make sure of this by only lowering pressure to the point that the actuator's ends collapse in a controlled way, causing them to act as telescopic pouches. This gives these actuators a stroke of about 15cm per end, 30cm overall (given Ø30cm tube).

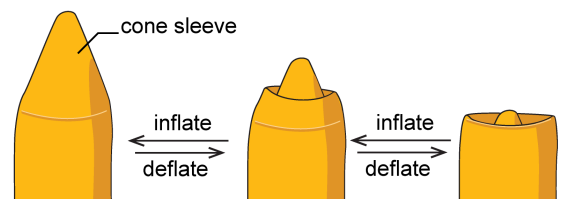


Figure 5: Telescoping actuators provide high force output. We achieve this through precise pressure control which prevents buckling and creates telescopic pouches.

We create this type of actuator from shorter tube segments (up to 1.2m at a Ø30cm diameter), as these are less prone to buckling. Our blowers are pressure-regulated, which allows for precise pressure adjustments without allowing the pressure to drop below a critical level thus preventing buckling.

As we show in the Section "Actuator Performance", integrated telescoping actuators are capable of producing significantly higher force than the buckling actuators. The main use case of telescoping actuators, therefore, is to literally do the heavy lifting, such as to lift a person on a motion platform, as shown Figure 1.

Optionally, for increased control and a longer stroke, we pull a separate conical sleeve (Figure 8c) over the ends of the integrated telescoping actuator segment. This allows for a longer stroke of up to 40cm per end and creates a favorable linear force profile (as shown in Figure 21c). This works since the cone shape causes the area that the air pressure acts on to scale linearly as the actuator extends. The taper of the sleeve governs the stroke length. Sleeves are pulled over the tube before assembly or added later and heat-sealed from the outside.

4.3 Integrated Muscle Actuator

When applying a *tensile* load to a pneumatic segment, we obtain a very different effect, namely, the effort of the aforementioned artificial muscle. The integrated muscle actuator allows us to produce models that actuate by means of tension. As shown in Figure 6 we use this to actuate the tail of an animatronic T-Rex sculpture (see Figure 2). Here, we implemented the T-Rex's back as an integrated muscle actuator. As shown, when empty, the segment is stretched to its full extent under the weight of the tail. However, upon inflation, the segment gains in width, and what it gains in width is lost in length, causing the actuator to contract, thereby lifting the load.

With our tube diameter of $\emptyset 30$ cm, we obtain 2 x 8.6 = 17.2cm of shrinkage upon inflating a segment, independently of the length of the tube. As shown, we therefore maximize the stroke of the actuator by subdividing the actuator into a sequence of segments. We achieve this by adding ties to the actuator, typically with regular spacing. To allow the actuator to operate using a single blower, we use loose ties of 10cm (4") diameter that allow for airflow.

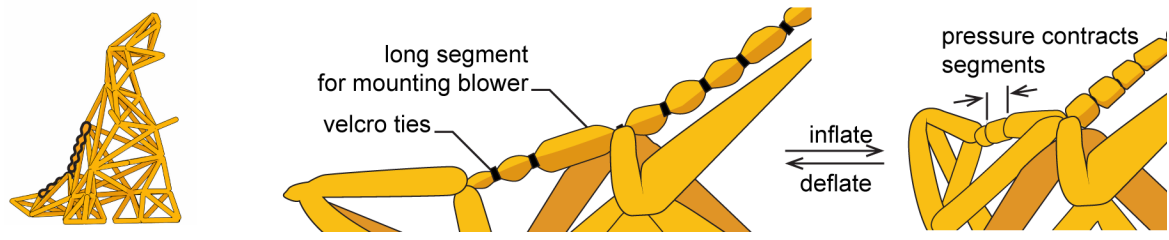


Figure 6: This integrated muscle actuator allows the T-Rex from Figure 2 to lift its tail when pressurized.

4.4 Creating a Restoring Force

 $\begin{array}{c} 236 \\ 237 \end{array}$

Our integrated actuators exert a force in only one direction, i.e., they are *single-acting*. As illustrated by Figure 7a, when the buckling actuator deflates, we may produce a matching *restoring force* by (b) relying on gravity. However, when gravity cannot be used, i.e., when perfectly horizontal left-right action is required, we may instead use (c) a second antagonistic actuator.

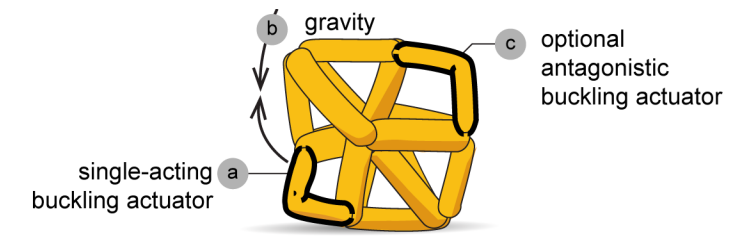


Figure 7: It is possible to restore the movement of the shown (a) buckling actuator either by (b) gravity or (c) a second, antagonistic actuator.

AirForce's single tube structures also offer a third option for generating a restoring force: as illustrated by Figure 8a the tube segments overlap at the node, which pushes segments away from each other. In most cases, this overlap is undesirable, as it applies torque to the adjacent tube segments, creating the risk of unintentional buckling. (b) We tend to suppress this by adding an additional short segment that loops around the node or by (c) covering tube segment ends in sleeves. However, we can also use the effect to serve as a restoring force. (d) An additional way to relieve unwanted force from nodes is to introduce an additional node that allows the tube to bend at sharp angles. We demonstrate this by fabricating a mattress for added safety under the motion platform (shown in Figure 1)

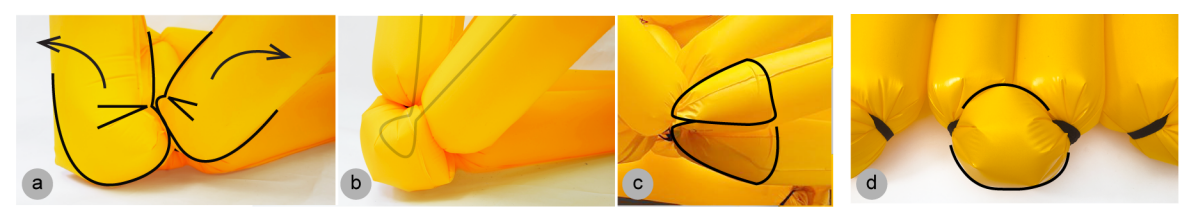


Figure 8: (a) Tube segments push each other out at nodes. (b) We bypass this either by adding an additional short segment that loops around or by (c) covering tube segment ends in sleeves or by (d) introducing an additional node (used in mattress from Figure 1).

4.5 Turning a Segment into an Actuator

The main benefits of AirForce's actuators derive from their integration into single tube structures. We will go into detail on fabrication in the following two sections. As a preview, however, Figure 9 shows how actuators (of any of the three

kinds) integrate: given a prefabricated segment of single tube structure, (a) users seal off the left and (b) right end of a respective tube segment. They make the seals airtight by running the tube through a tie *twice*. (c) Users now create an incision, insert one of our custom inlets, and attach one of our custom blowers.



Figure 9: Users turn a truss segment into any type of integrated actuator by adding four components (a-d).

5 THE TECHNICAL COMPONENTS OF AIRFORCE

Before we present how users create *their specific* structures, we show how users fabricate the required generic and reusable components, i.e., custom blowers, custom inlets, and tubes suitable for the resulting high pressure.

5.1 Custom Blower: Casing, Mount, and Pressure Control

Actuators require compressed air. Conventional compressors (e.g., [40]) cannot provide the flow rate required to actuate our three actuator types at reasonable speeds (and their flow rate drops further once their comparably small reservoirs (e.g., 64 liters [40]) are exhausted). AirForce therefore, uses *dynamic* compressors, also known as *blowers* [29].

For our custom blower design, we use a *Domel 714* [5] series blower motor, which is capable of providing up to 250mbar air pressure at 36V (350 mbar with fully charged 42V batteries). This pressure, applied to a 30cm diameter integrated telescoping actuator, will result in 1767N expansion force, i.e., capable of pushing ~180kg of load.

As illustrated by Figure 10a, AirForce packages blowers into standalone untethered *blower modules* with a 3D-printed housing. The housing holds the battery, the controller board, and the blower motor, guiding pressurized air into a nozzle. The nozzle is made from flexible PVC tubing and contains a pressure sensor. Figure 10b shows the custom printed circuit board. Designed around an *ESP32C3* microcontroller (*Seedstudio XIAO*). The firmware of this board receives commands from our control app (see Section 6.4) via Wi-Fi and, in response, controls the blower motor's power using a pulse-width modulated signal.

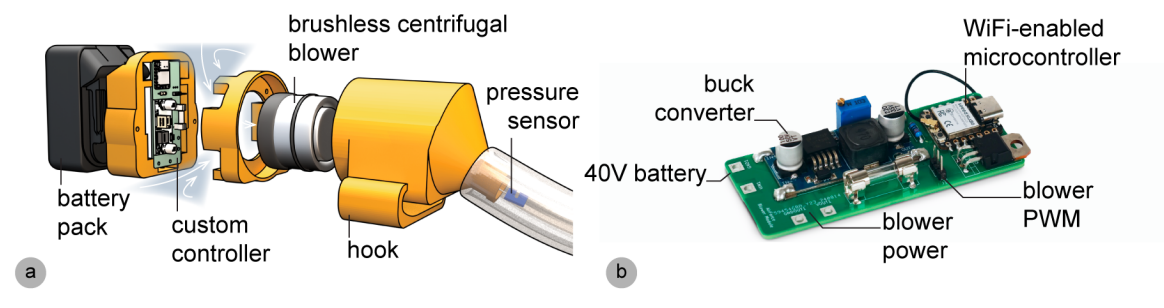


Figure 10: (a) Custom 3D-printed blower module. (b) The custom printed circuit board allows controlling blowers remotely via Wi-Fi.

To achieve precise force control of our actuators, the blowers implement a pressure feedback loop using an *Adafruit MPRLS 3965* pressure sensor. We have implemented and tuned a custom PID algorithm to keep the pressure at the desired levels, despite external disturbances. The blowers support a direct PWM control as well.

The unit is powered by a 40V, 2.5Ah battery pack (*Makita Corporation BL4025*) that allows for 15-45 minutes of operation, depending on required pressure. The PID pressure control also helps here, increasing the battery life by reducing power when the desired pressure is reached.

One of the limitations of our blower design is that it can only passively deflate the structure by stopping the motor, allowing air to exhaust back through the blower, as these types of centrifugal blowers cannot be reversed.

5.2 Custom Inlet Made from Tube Material

To make sure there is no pressure loss between the blower and the tube, users mount blowers by means of an inlet. As shown in Figure 11, our custom inlets are made from tube material. (b) At the marked location, users cut the top layer of the tube using a knife designed to produce a shallow slit (a so-called kiss-*cut* knife). (c) Users then insert the valve and permanently attach it either using double-sided adhesive tape or liquid rubber adhesive (e.g., kövulfix).



Figure 11: Users mount a custom inlet by (a) cutting, (b) inserting, and (c) gluing.

Our valve design builds on a *Heimlich Valve* [9], which is a one-way valve design that pumps air through a nozzle made from two parallel sheets of material inside a pneumatic cavity. As shown in Figure 12a, the design allows for airflow inwards, which spreads the two sheets. Reversing the airflow presses the two sheets together, sealing the inlet.

We adapted this general design for integration into single-tube structures, as shown in Figure 12a. The main benefit of our adapted design is that it can be mounted into an already completed single-tube structure, (b) as mounting the inlet only requires access from the *outside* of the tube. This is crucial, as AirForce may employ very long tubes (the T-Rex shown in Figure 2 uses 250m of tube), thus making it challenging to mount valves that require accessing the *inside* of the tube.

Our inlet is made from the same TPU-coated nylon fabric as our tube structures; one side of it features a heat-sealing coating. As illustrated by Figure 12c, users fabricate an inlet by overlaying two strips with the heat-sealable side facing each other, welding it at both sides to form a small tube, but leaving the top open to fabricate a flap for connecting it to the tube. Using the valve as is would result in small leakages when mounting it in a slit on the tube. (d) Therefore, users cut away a small strip *on the sealing line*, fold it up, and glue it to the flap. This way the inlet has a flat surface for mounting it to the tube using double-sided tape or adhesive. Additionally, a loop gets heat-sealed onto mount the blower.

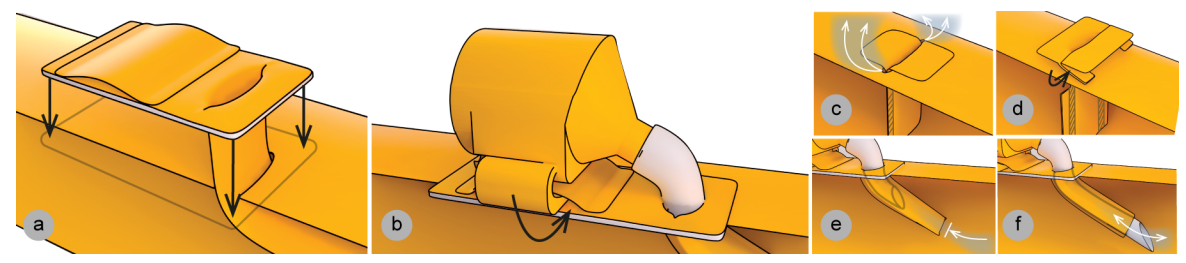


Figure 12: (a) The inlet is designed to be installed from the outside of the tube using adhesive. (b) It includes a fabric loop to mount the blower unit. (c-d) The design is based on a Heimlich valve that we extend to work without leakages. Blowers that inflate static segments use (e) a short nozzle which acts a one-way check valve to keep them pressurized, while blowers that power an actuator, use (f) a long nozzle, which keeps the inlet open and allows for air to flow back out on the actuator.

For static structures, we use the design shown in Figure 12e. Its one-way nature maintains pressure, even when blowers are off. The design also allows inflating part of a structure, pulling the blower out (which closes the inlet), and then using the same blower to inflate a different segment. (f) For use with actuators, we use blowers with a *longer* nozzle. Inserting the blower now keeps the flap open and allows for bi-directional airflow, which allows blowers to inflate *and deflate*. However, as before, removing a blower closes the valves. This is useful during repair or when abandoning an actuator location after redesigning the structure.

5.3 Tube Redesign for High Pressure

AirForce uses a similar tube material as AirTied [40], i.e., *Rivertex Ecoseal 200* [42]. It combines a 235den woven nylon fabric that takes up the tension with a single-sided coating of heat-sealable Thermoplastic Polyurethane.

However, to make the resulting structures strong enough to lift humans, we increase the tube diameter from Ø13cm to Ø30cm, which increases the maximum load quadratically ($F=A\cdot P$, $A=r^2\pi$), thus by about a factor of 4x.

To accommodate the increased tension, we redesigned the tube construction, as illustrated by Figure 13: (a) AirTied (as well as *Aeromorph* [38], *Printflatables* [45]) use *fin seals* along the seam. This places all the load on the inner edge of the seam. The inner seam forms a *line*, and thus this design runs the risk of *peeling* open when high pressure is applied [33]. (b) We therefore switch to *lap seals*. Since lap seals distribute the load across an *area*, this raises the maximum permissible pressure of the seals beyond the tensile strength of the fabric. (c) Since only one side of our tube material is heat-sealable, we update our design to use two distinct strips of material, one of which, if flipped inside-out, allows the heat-sealable surfaces of both strips to be fused.

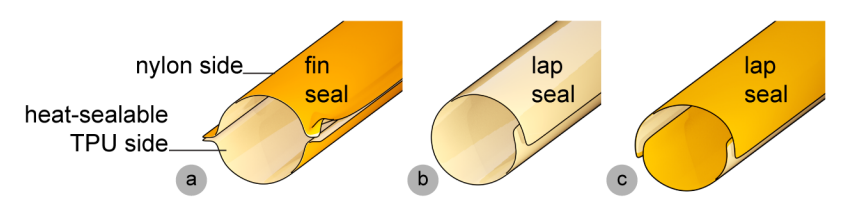


Figure 13: (a) The seams of fin seals peel away under pressure. (b) Lap seals are more robust. (c) AirForce makes lap seals from *two* strips to achieve lap seals with fabrics that have a heat-sealable coating (here: light yellow) on one side only.

It is possible to seal the tube manually using an iron and a rubberized roller. If available, is it possible to use a specialized machine shown in Figure 14 (*Leister HEMTEK ST [18]*). The device allows sealing the tube using a 2.3kW heat gun. The pressure rollers apply pressure and guide the material. This allows us to seal 90m of tube per hour. (Fabricating the tube for the motion platform shown in Figure 1 takes 6min; the T-Rex from Figure 2 takes less than 3h).

We feed the shown setup with two strips of material, both with the adhesive side up, but with 4cm of the bottom sheet exposed. We feed this stack of two sheets through a custom spiral-shaped jig, which folds 2cm from the bottom of the top sheet, thereby aligning them to be heat-sealed by the device.

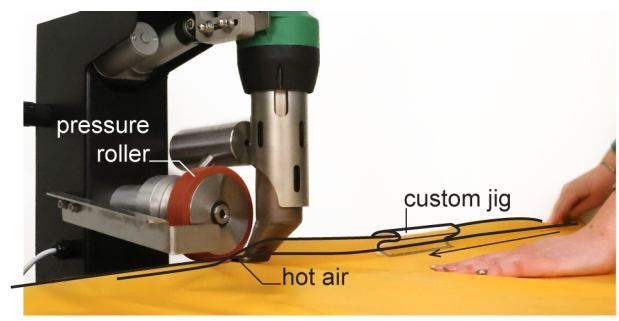


Figure 14: Our setup based on the *Leister HEMTEK ST* [18] heat sealing device. Our custom jig is key to aligning the adhesive sides of the two sheets which allows making a 90m tube per hour.

5.4 Node and Seals

While single-tube structures have previously been tied using wire ties [40], given the increased tube size and pressure of the AirForce designs, we switched to Velcro straps (2cm wide *Velcro Brand Back To Back Tape* [55]). Velcro ties are durable, do not damage the tubes, and are easy to apply and remove by hand.

As illustrated in Figure 15, to combine two (or more) tubes into a node, (a) we first constrict each tube using a strap of Velcro tape, and then (b) use a third strap to connect the first two straps. To restrict air flow into or out of the actuator segment, (c) we form air-flow-blocking loops, and (d) finally combine the loops with other nodes.



Figure 15: (a-b) We construct regular, airflow-permitting nodes using Velcro ties. Adding (c-d) forming a loop and then feeding a Velcro strip through blocks airflow at nodes next to the actuators.

6 FABRICATING A CUSTOM ANIMATRONICS STRUCTURE

Given components as described in the previous section, users are able to now design their own large-scale animatronics structures using the following four-step process.

6.1 Step 1: Design Structure using our Blender Extension

Users start by designing the structure as a wireframe. They may use the open-source design tools *PneuMesh* [8], *Truss-Former* [13], or any other 3D editor capable of exporting 3D files in the .obj file format. To provide users also with the functionality required for actuators, we provide an AirForce plug-in for *Blender* [1], shown in Figure 16. (a) The plug-in allows users to convert segments into actuators and keeps users informed about the overall material cost and the number

of required blowers. (b) When complete, the plug-in creates an optimized single tube routing through the model, automatically determines blower positions (see Section "*Algorithm*").

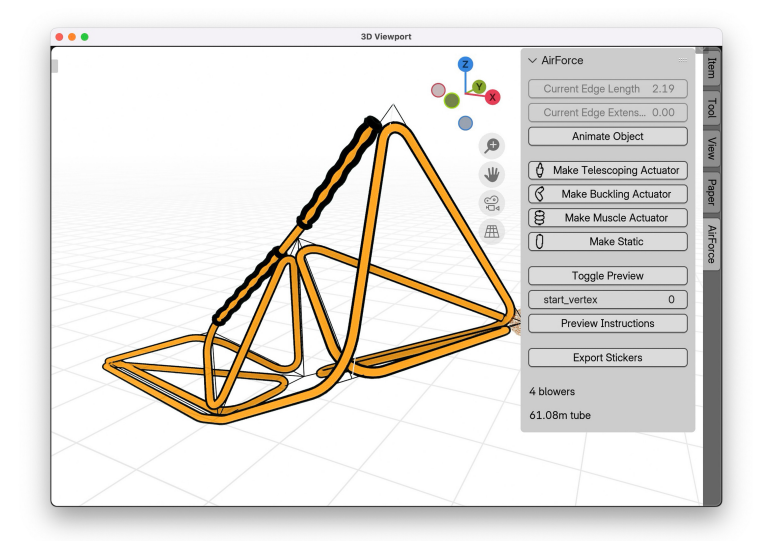


Figure 16: The AirForce plugin for *Blender* [1] allows users to create structures and place actuators. Here, we just added the muscle actuator (thick outline) to the T-Rex's tail from Figure 2.

6.2 Step 2: Print and Apply Assembly Instructions

When users click on "export", the plug-in automatically generates assembly instructions, including blower and seal positions. It exports the model in the form of "1D" assembly instructions, i.e., where along the single tube to tie a node, where to add a blower, and where to seal off the tube.

In theory, the resulting instructions could be fed into an automated tying machine (e.g., an *AirTied* [40] device scaled to double size), but to make the approach accessible to a wider audience without access to this assembly device, we here present a process that requires only manual tools and an inexpensive label printer:

As shown in Figure 17a, our plug-in controls a label printer (here, *Brother QL 700*) and produces five types of stickers, one sticker at a time. (b) Each sticker contains an action to perform (see below), and where along the tube to place the sticker (here expressed in meters from the beginning of the tube) and which blowers to use. Users apply the stickers to the tube at the indicated position by laying out the tube along a measuring tape or using a measuring roller.



Figure 17: (a) Our blender plug-in allows users to produce assembly instructions in the form of stickers, which (b) users apply to the single tube, at the locations stated on the labels.

6.3 Step 3: Users Construct Nodes and Add Blowers

Users create their structure following the instructions on the stickers. They begin by creating the topology of their structure: In order to create the nodes, users assemble all spots that show the same node ID and tie them up using Velcro ties as described earlier. An additional 'seal' on the stickers indicates that the respective node is supposed to be air-tight, as it is adjacent to an actuator, in which case users use a metal cuff instead of the Velcro tape (see Figure 15a).

An animated preview in AirForce's Blender plugin traces the single tube along its path, providing users with an additional overview of the fabrication process.

Users then construct the actuators, which at this point is straightforward: following the instructions on the stickers, they insert blowers and clip them into the straps that are part of the inlets.

6.4 Step 4: Inflate and Control

Finally, we provide users with the simple smartphone app shown in Figure 18, which allows them to control the actuators inside their structure by communicating with the WiFi modules embedded in the blowers' custom controllers. For blowers that users classify as "actuators", the app offers a slider to control their pressure and to name blowers, such as 'head up' or 'tail left'; for "static" blowers, the app offers only on/off toggles. The app also allows connecting MIDI devices. Here, we use a MIDI-based board with audio faders to control the T-Rex, as shown in Figure 2.



Figure 18: (a) The simple AirForce control app. (b) The app also allows users to control their structure using audio faders via MIDI.

Actual applications instead talk to the blowers using our Python library. The motion platform in Figure 1, for example, syncs the motion platform movements to a 360° VR video of a rollercoaster ride. The player is implemented using JavaScript and WebXR and sends the video playback progress periodically to a Python web server. The player reads tuples formatted like 15: [0.3, 1.0, 1.0, 1.0, 1.0, 1.0] to indicate that at second 15, all actuators except the first one are fully extended, while the first one is powered at 30%, tilting the user to the right. Finally, it sends the respective commands via WiFi and UDP to the respective blower.

6.5 Step 5: Disassemble and Reuse Material

AirForce structures are fully reusable. Removing ties turns any structure back into a single tube (see AirTied [42]); inlets self-seal, i.e., old inlets can stay without causing leakage. Velcro ties and blowers are reusable. Making a new model thus only requires adding new inlets.

7 STRUCTURE GENERATION ALGORITHM

The export algorithm in AirForce's blender plug-in converts 3D truss models into single tube structures. Similar to AirTied's algorithm [40], the objective of this algorithm is to find the tube path that traverses the model's edges (a so-called *Eulerian path*) while requiring only the minimum number of edges to be traced twice. Unlike AirTied's algorithm, however, the AirForce algorithm also needs to handle actuators, which are tube segments that are sealed off from the

rest of the segments. This creates additional optimization constraints, namely, to minimize the required number of blowers for separated static segments.

Figure 19 illustrates this problem at the example of a motion platform, the vertical members of which are telescoping actuators, while the top triangle is inflated statically. (a) Naïvely running the algorithm from related work traverses the three static segments (the top triangle) in random order. Since these segments come into contact with actuators, they must be sealed off and thus need three blowers of their own to inflate them. (b) Our optimized route traverses these static segments in succession and thus unifies them, requiring only one blower for the connected static segments. This saves time and cost.

The AirForce blender plugin creates a tube routing that minimizes blowers and generates assembly instructions in a three-step process.

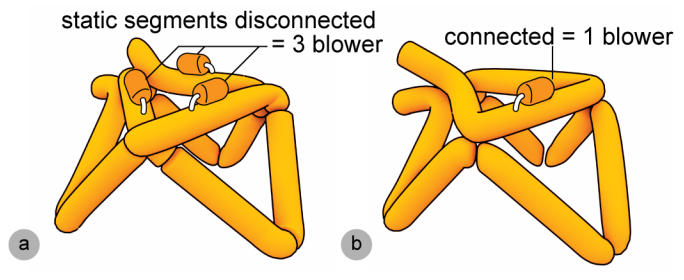


Figure 19: (a) The AirForce Algorithm reduces the number of blowers required from the static segments from three to (b) one. It achieves this by routing the tube to traverse the static segments in succession, unifying them into one group.

7.1 Step 1: Routing the Tube to Minimize the Number of Blowers

To find an optimal path, our algorithm traverses the graph of the input model step-by-step and returns the order of nodes as a fabrication sequence. It starts at a node which is at an end of an actuator segment to avoid splitting connected groups of static segments in two, as this would require an additional blower.

The AirForce algorithm then chooses the next edge according to the following criteria, in descending priority: (1) The next edge should not "disconnect" the model, i.e., it should not leave edges behind that are disconnected from the rest of the model, (2) if the last edge was a static edge, the next edge should also be a static edge. If none of these criteria are met, a random edge is picked.

Our algorithm uses a randomized greedy approach, running iteratively until it converges. To avoid suboptimal results, we perform probabilistic boosting, rerunning with random starting nodes and tie breakers for the edge selection (we used 100 reruns in our experiments). The solution with the fewest blowers and seals is then returned to the user. Before traversing the model, we add additional double edges to ensure that it is traversable by a single tube using NetworkX' *Eulerize* algorithm [31]. This inserts double edges where necessary.

7.2 Step 2: Place Blowers

 The AirForce algorithm places one blower for every actuator. Due to the path routing, double edges may be placed by the algorithm in parallel to actuators. In this case, we only place one blower on the actuator and leave the second edge sealed off without a blower, thus remaining permanently deflated. For connected static segments, we place one blower in the middle of the static groups.

7.3 Step 3: Render Stickers and Assembly instructions

- 431 Finally, the plugin generates instructions to fabricate the structure. As mentioned previously these are in the form of
- 432 stickers that will be placed along the tube by the user beforehand. An image is generated for each instance of a feature
- 433 such as where to constrict the tube, which segments to seal-off, where to attach blowers, etc. In addition, we also gen-
- 434 erate a sequence of images that show the model at each assembly step for users to compare to during assembly.

8 EVALUATION

- 436 To evaluate our actuator design, we tested the force output and response time of our actuators, ran a user study to
- 437 estimate fabrication time and fabricated two full models, a motion platform, and a 16m long, 8m high T-Rex animatronics
- 438 sculpture.

430

435

439

8.1 Technical Evaluation of Actuator Performance

- The key to animating AirForce's structures lies in the actuators' ability to lift the expected load. To help users choose
- the right actuators for the desired motion, we conducted a series of load tests with all three of our actuator types.
- To measure the force response of each actuator, we fixed the endpoints of the actuators in an aluminum frame with
- a height-adjustable upper carriage. The force gauge was used to complete a series of measurements at discrete actuator
- 444 extension levels. All tests were repeated with three pressure values of 100, 150, and 200mbar. To keep pressure constant
- 445 during the measurements, we used our custom PID-controlled blowers. For measurements, we used an Ailigu ZP digital
- 446 dynamometer force gauge and a Senseca ECO 240-2 pressure gauge. The tube diameter in all the cases was Ø30cm. All
- 447 experiments were conducted with up to 200mbar pressure; our tube actuators can take even larger pressures. These
- 448 forces can be approximately extrapolated from the experiments below.
- 449 **Bucking actuator**: Figure 20a shows the test setup and measurement results of our buckling tube actuator. We tested
- 450 a shorter 1.5m actuator, as well as a 2.5m actuator. As shown in the force diagrams, increasing the actuator length
- 451 proportionally decreases the force. The maximum force these actuators could exert was (b) 480N and (c) 280N, respec-
- 452 tively (at 200mbar, 120° angle). However, we note that the buckling actuators have a local minimum in their force profile
- at around a 60° angle, so this minimum must be considered when sizing the actuator.
- 454 Figure 20d shows the response time of a 75cm buckling actuator. It reaches its maximum pressure and force of output
- 455 of 404N in about 1.88s. Deflation is somewhat slower, about 6 seconds, due to its passive nature. Both these values are
- dependent on the tube volume.

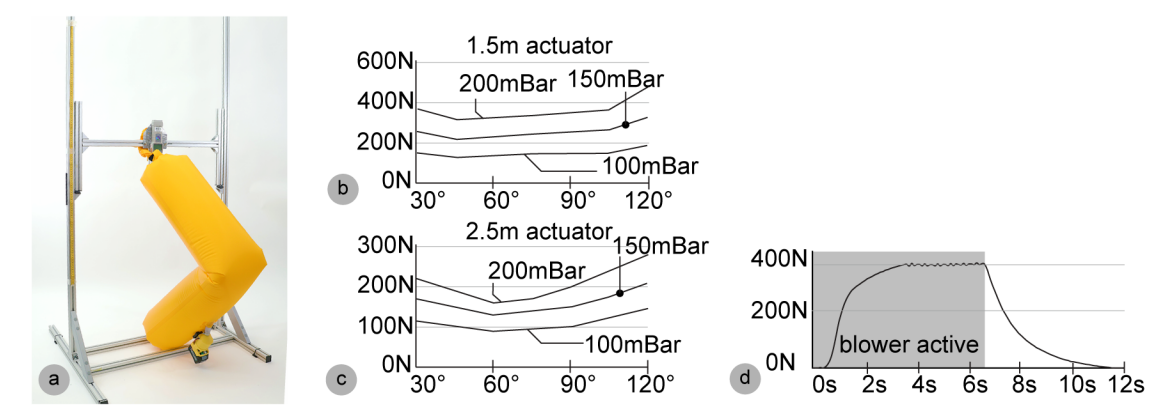


Figure 20: (a) Integrated buckling actuator and (b, c) performance (force vs angle). We highlight that increasing the actuator length proportionally decreases the force. (d) The response time of a 75cm buckling actuator is about 2s.

Telescoping Actuator: Figure 21 shows the telescoping actuator test. We tested this actuator type in two variations: (a) with its natural dome ending and (b) also with constricting cone sleeves on both ends, which creates a longer stroke and a more linear force profile.

This type of actuator creates significantly higher forces than the previous buckling type (max. 1400N at 200mbar); however, the stroke is much shorter. With a natural dome ending, the force ramps up nonlinearly and reaches its maximum already after about 20 cm compression. However, this stroke can be significantly enlarged by adding a constricting sleeve on both ends (here 40 cm long) that proportionally reduces the diameter from 30cm to 10cm. This also makes the force profile linear as seen in Figure 21c. The limitation of this technique is that it makes the actuator more susceptible to unwanted buckling at the ends in the presence of sideways forces.

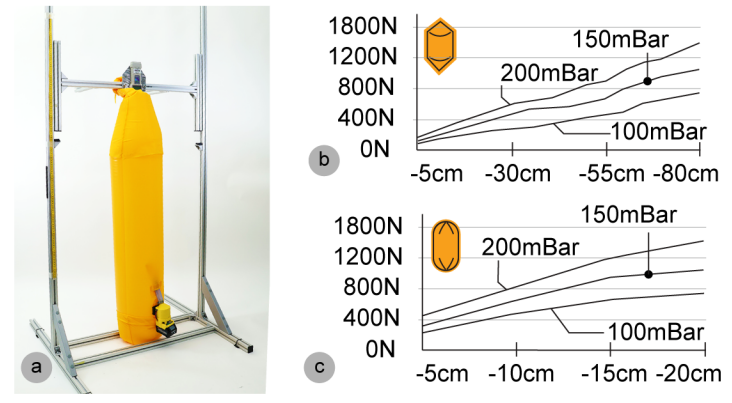


Figure 21: (a) Integrated telescoping actuator test setup. (b) Force curve with natural dome-shaped endings, and (c) with added cone-shaped sleeve constrictions.

Muscle Actuator: The test setup for the artificial muscle-type actuator is shown in Figure 22a. The nominal length of the actuator was 2m in the relaxed state and could be contracted to about 145cm. The highest force was measured in the fully extended state, reaching 2330N at 200mbar. As is visible from the diagram, the force linearly decreases along the stroke. It is possible to increase the stroke by adding more constriction points,; however, the spacing between them should remain larger than ~34cm to be able to reach the natural rounding.

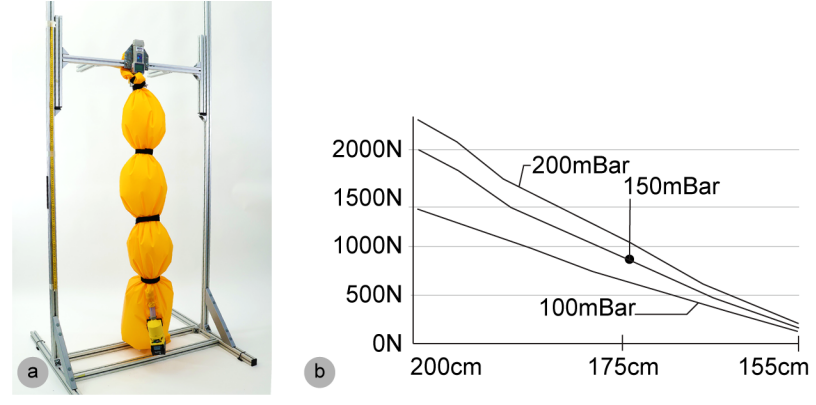


Figure 22: (a) Integrated muscle actuator test results in a (b) linear force profile.

8.2 User Study to Estimate Fabrication Time

To understand how long it takes for users to fabricate AirForce structures we conducted a simple user study.

Procedure: We picked our most complex subassembly, the head of the 8m T-Rex from Figure 2 (2x3x5 m, 11 nodes and 24 edges), and the only challenging subtask, i.e., tying up the (labeled and Velcro-segmented) tube into the 3D model. We provided participants with a 24-image sequence showing increasingly longer pieces of tube (auto-generated using our Blender plugin). Before starting the study, we laid out the prepared tube in a zig-zag pattern with the start node facing the participant and walked them through the instruction manual beforehand. During assembly, we handed them Velcro strips and answered any questions that came up. If they deviated from the printed instructions, we informed them about their mistake. We stopped the time once the participant finished the last connection. At the end, they filled out questions on demographics and ease of assembly.



Figure 23: (a) The participants (here, P1) start with a tube with ties and stickers in front of them. (b) Then, they follow the assembly instructions until they connect the last segment and complete their task. (c) The result is an inflatable dinosaur head.

Participants: We recruited 12 participants (11 male, 1 female, average age 23.3, σ = 3.1) without prior assembly experience from our institution.

Results: All participants assembled the structure successfully, taking on average 24:20min (σ = 9:37min), and rated ease of assembly as 4.7/7 in our questionnaire.

Discussion: To approximate overall assembly time using this data, we assume that the assembly effort scales linearly with the number of edges. This gives us $24:20\min/24$ edges = $\sim1\min/edge$ for assembly. For the complete fabrication process, we need to consider steps taken before assembly, i.e., printing stickers and applying them at the measured position. When preparing the study, we measured, and these tasks took 30 minutes for 24 edges, resulting in another ~1 minute/edge. Finally, adding a blower and inlet took 10 minutes/blower. This gives us an estimation of t = 2min * edges

- + 10min * blowers. For the head (24 edges, 2 blowers), this results in 1 hours and 8 minutes of end-to-end fabrication
- 502 time. Extrapolating to the entire T-Rex (108 edges, 7 blowers), it would approximately take 4 hours and 46 minutes.
- This is comparable to the manual labor required for TrussFormer [14] but does not require more than 100 hours of
- 504 prior 3D printing for a similar object, significantly shortening the time from design to structure.

8.3 Applications

- 506 The 8m high animatronic T-Rex sculpture, shown in Figure 2, uses 250m of tube, contains 37 nodes, 108 edges, and is
- actuated using 11 blower modules. The design can open and close its jaw using a buckling actuator and lift its tail using
- an integrated muscle actuator in its back. It is secured with water-filled umbrella stands.
- The motion platform uses 10m of tube and consists of 7 nodes, nine edges, and six actuators, resulting in 7 blowers.
- We anchor the motion platform with a mattress made from a tube and connect the bottom nodes with velcro strips to
- 511 form a triangle.

505

512

519

522

9 CONCLUSION

- 513 In this paper, we presented AirForce, a system that fabricates actuated human-scale truss structures. We integrate our
- 514 actuators into single-tube structures, which gives us a range of benefits, including efficient single user assembly, 100%
- 515 reusability of the tube by unfolding and refolding the structure, easy transport and setup, and excellent strength-to-
- weight ratio which allows lifting human weight while being a human-safe.
- As future work, we plan to explore how the tube structures presented in this paper might allow us to create the
- elements required for mass-spring-damper systems.

Acknowledgement

520 <anonymized for review>

521 References

- [1] Blender Foundation. 2025. blender. Retrieved from blender.org
- 523 [2] Anke Brocker, Jakob Strüver, Simon Voelker, and Jan Borchers. 2022. SoRoCAD: A Design Tool for the Building Blocks of Pneumatic Soft Robot-524 ics. In Extended Abstracts of the 2022 CHI Conference on Human Factors in Computing Systems (CHI EA '22), April 28, 2022. Association for 525 Computing Machinery, New York, NY, USA, 1–7. https://doi.org/10.1145/3491101.3519770
- 526 [3] John Chilton. 1999. Space Grid Structures. Taylor & Francis Ltd.
- 527 [4] Raphael Deimel and Oliver Brock. 2013. A compliant hand based on a novel pneumatic actuator. In 2013 IEEE International Conference on Robotics and Automation, 2047–2053. DOI:https://doi.org/10.1109/ICRA.2013.6630851
- 529 [5] Domel, d.o.o. 714 Thruflow high speed and compact Brushless vacuum motors. Retrieved from https://www.domel.com/product/714-thruflow-high-speed-and-compact-103
- 531 [6] Festo Corporation. Fluidic Muscle DMSP. Retrieved from https://www.festo.com/us/en/p/fluidic-muscle-id_DMSP/
- 532 [7] Joseph D. Greer, Tania K. Morimoto, Allison M. Okamura, and Elliot W. Hawkes. 2017. Series Pneumatic Artificial Muscles (sPAMs) and Application to a Soft Continuum Robot. IEEE Int Conf Robot Autom 2017, (2017), 5503–5510. https://doi.org/10.1109/ICRA.2017.7989648
- 534 [8] Jianzhe Gu, Yuyu Lin, Qiang Cui, Xiaoqian Li, Jiaji Li, Lingyun Sun, Cheng Yao, Fangtian Ying, Guanyun Wang, and Lining Yao. 2022. PneuMesh: 535 Pneumatic-driven Truss-based Shape Changing System. In *Proceedings of the 2022 CHI Conference on Human Factors in Computing Systems* (CHI '22), Association for Computing Machinery, New York, NY, USA, 1–12. DOI:https://doi.org/10.1145/3491102.3502099
- 537 [9] Henry J. Heimlich. 1968. Valve Drainage of the Pleural Cavity. Dis Chest 53, 3 (March 1968), 282–287. DOI:https://doi.org/10.1378/chest.53.3.282
- 538 [10] Ozgun Kilic Afsar, Ali Shtarbanov, Hila Mor, Ken Nakagaki, Jack Forman, Karen Modrei, Seung Hee Jeong, Klas Hjort, Kristina Höök, and Hiroshi
 539 Ishii. 2021. OmniFiber: Integrated Fluidic Fiber Actuators for Weaving Movement based Interactions into the 'Fabric of Everyday Life.' In The 34th
 540 Annual ACM Symposium on User Interface Software and Technology (UIST '21), October 12, 2021. Association for Computing Machinery, New York,
 541 NY, USA, 1010-1026. https://doi.org/10.1145/3472749.3474802
- 542 [11] Marirena Kladeftira, Matthias Leschok, Eleni Skevaki, and Yael Ifrah. 2021. Digital Bamboo. *Biennale Architettura 2021*, Venice, Italy. Retrieved from https://dbt.arch.ethz.ch/project/digital-bamboo/

- 544 [12] Ryota Kobayashi, Hiroyuki Nabae, Gen Endo, and Koichi Suzumori. 2022. Soft Tensegrity Robot Driven by Thin Artificial Muscles for the Exploration of Unknown Spatial Configurations. *IEEE Robotics and Automation Letters* 7, 2 (April 2022), 5349–5356.
 546 https://doi.org/10.1109/LRA.2022.3153700
- 547 [13] Robert Kovacs, Alexandra Ion, Pedro Lopes, Tim Oesterreich, Johannes Filter, Philipp Otto, Tobias Arndt, Nico Ring, Melvin Witte, Anton Syny-548 tsia, and Patrick Baudisch. 2018. TrussFormer: 3D Printing Large Kinetic Structures. In Proceedings of the 31st Annual ACM Symposium on User 549 Interface Software and Technology (UIST '18), Association for Computing Machinery, New York, NY, USA, 113–125. 550 DOI:https://doi.org/10.1145/3242587.3242607
 - [14] Robert Kovacs, Anna Seufert, Ludwig Wall, Hsiang-Ting Chen, Florian Meinel, Willi Müller, Sijing You, Maximilian Brehm, Jonathan Striebel, Yannis Kommana, Alexander Popiak, Thomas Bläsius, and Patrick Baudisch. 2017. TrussFab: Fabricating Sturdy Large-Scale Structures on Desktop 3D Printers. In Proceedings of the 2017 CHI Conference on Human Factors in Computing Systems (CHI '17), Mai 2017. Association for Computing Machinery, New York, NY, USA, 2606–2616. https://doi.org/10.1145/3025453.3026016
 - [15] Kohei Kurita, Fumihiro Inoue, Noriyuki Furuya, Takashi Shiokawa, and Michihiro Natori. 2001. Development of Adaptive Roof Structure by Variable Geometry Truss. September 12, 2001. Krakow, Poland. https://doi.org/10.22260/ISARC2001/0012
 - [16] Babar Jamil, Namsoo Oh, Jin-Gyu Lee, Haneol Lee, and Hugo Rodrigue. 2024. A Review and Comparison of Linear Pneumatic Artificial Muscles. Int. J. of Precis. Eng. and Manuf.-Green Tech. 11, 1 (January 2024), 277–289. https://doi.org/10.1007/s40684-023-00531-6
 - [17] Haneol Lee and Hugo Rodrigue. 2023. Harnessing the nonlinear properties of buckling inflatable tubes for complex robotic behaviors. *Materials Today* 63, (March 2023), 59–88. https://doi.org/10.1016/j.mattod.2023.02.005
 - [18] Leister HEMTEK ST, 230V/2350W, 20mm, CEE 3/16 | 157.868. Retrieved April 8, 2025 from https://www.leister.com/en/product/Hemtek-ST/157-868
 - [19] Yuyu Lin, Jesse T Gonzalez, Zhitong Cui, Yash Rajeev Banka, and Alexandra Ion. 2024. ConeAct: A Multistable Actuator for Dynamic Materials. In Proceedings of the 2024 CHI Conference on Human Factors in Computing Systems (CHI '24), May 11, 2024. Association for Computing Machinery, New York, NY, USA, 1–16. https://doi.org/10.1145/3613904.3642949
 - [20] Michael J. Littlehorn. 1999. Balloon valve and method of producing. Retrieved from https://patents.google.com/patent/US5934310A/en
 - [21] Luke Lo. 2001. Inflation nozzle structure of an inflatable envelope. Retrieved from https://patents.google.com/patent/US6170513B1/en
- Giyuyu Lu, Tianyu Yu, Semina Yi, Yuran Ding, Haipeng Mi, and Lining Yao. 2023. Sustainflatable: Harvesting, Storing and Utilizing Ambient Energy for Pneumatic Morphing Interfaces. In *Proceedings of the 36th Annual ACM Symposium on User Interface Software and Technology (UIST '23*),
 October 29, 2023. Association for Computing Machinery, New York, NY, USA, 1–20. https://doi.org/10.1145/3586183.3606721
- 571 [23] Yiyue Luo, Kui Wu, Andrew Spielberg, Michael Foshey, Daniela Rus, Tomás Palacios, and Wojciech Matusik. 2022. Digital Fabrication of Pneumatic Actuators with Integrated Sensing by Machine Knitting. In Proceedings of the 2022 CHI Conference on Human Factors in Computing Systems
 573 (CHI '22), April 29, 2022. Association for Computing Machinery, New York, NY, USA, 1–13. https://doi.org/10.1145/3491102.3517577
 - [24] Andreas Lyder, Ricardo Franco Mendoza Garcia, and Kasper Stoy. 2008. Mechanical design of odin, an extendable heterogeneous deformable modular robot. In 2008 IEEE/RSJ International Conference on Intelligent Robots and Systems, September 2008. 883–888. https://doi.org/10.1109/IROS.2008.4650888
- 577 [25] Chico MacMurtrie. Border Crossers. Retrieved from https://amorphicrobotworks.org/border-crossers

551

552

553

554

555

556

557

558

559

560

561

562563

564

565

566

567

574

575

576

578

579

580

585

- [26] MERO-TSK International GmbH & Co. KG. MERO. Retrieved from https://www.mero.de/en/
- [27] Koryo Miura, Hiroshi Furuya, and Kenichi Suzuki. 1985. Variable geometry truss and its application to deployable truss and space crane arm. Acta Astronautica 12, 7 (July 1985), 599–607. DOI:https://doi.org/10.1016/0094-5765(85)90131-6
- 581 [28] Takafumi Morita, Ziyuan Jiang, Kanon Aoyama, Ayato Minaminosono, Yu Kuwajima, Naoki Hosoya, Shingo Maeda, and Yasuaki Kakehi. 2023.
 582 InflatableMod: Untethered and Reconfigurable Inflatable Modules for Tabletop-sized Pneumatic Physical Interfaces. In Proceedings of the 2023 CHI
 583 Conference on Human Factors in Computing Systems (CHI '23), April 19, 2023. Association for Computing Machinery, New York, NY, USA, 1–15.
 584 https://doi.org/10.1145/3544548.3581353
 - [29] Hubertus Murrenhoff and Olivier Reinertz. 2016. Fundamentals of Fluid Power: Part 2: Pneumatics (2nd edition ed.). Shaker.
- 586 [30] Koya Narumi, Hiroki Sato, Kenichi Nakahara, Young ah Seong, Kunihiko Morinaga, Yasuaki Kakehi, Ryuma Niiyama, and Yoshihiro Kawahara.
 587 2020. Liquid Pouch Motors: Printable Planar Actuators Driven by Liquid-to-Gas Phase Change for Shape-Changing Interfaces. IEEE Robotics and
 588 Automation Letters 5, 3 (July 2020), 3915–3922. https://doi.org/10.1109/LRA.2020.2983681
- 589 [31] NetworkX developers. Eulerize. 3.4.2 documentation. Retrieved from https://networkx.org/documentation/stable/reference/algorithms/gener-590 ated/networkx.algorithms.euler.eulerize.html
- 591 [32] Pham Huy Nguyen and Wenlong Zhang. 2020. Design and Computational Modeling of Fabric Soft Pneumatic Actuators for Wearable Assistive
 592 Devices. Sci Rep 10, 1 (June 2020), 9638. https://doi.org/10.1038/s41598-020-65003-2
- 593 [33] Namsoo Oh and Hugo Rodrigue. 2023. Toward the Development of Large-Scale Inflatable Robotic Arms Using Hot Air Welding. Soft Robotics 10, 1 (February 2023), 88–96. https://doi.org/10.1089/soro.2021.0134
- 595 [34] Sora Oka, Kazuki Koyama, Tomoyuki Gondo, Yasushi Ikeda, Yoshihiro Kawahara, and Koya Narumi. 2024. Folding Angle Control of Inter-Connected Pouch Motors. In Extended Abstracts of the CHI Conference on Human Factors in Computing Systems, May 11, 2024. ACM, Honolulu HI USA, 1–4. https://doi.org/10.1145/3613905.3648640
- 598 [35] Sora Oka, Kazuki Koyama, Tomoyuki Gondo, Yasushi Ikeda, Yoshihiro Kawahara, and Koya Narumi. 2025. Pneumatic Laser Origami: Rapid and Large-Scale Fabrication of Laser-Welded Pouch Motors for Shape-Changing Products. In *Proceedings of the Nineteenth International Conference on Tangible, Embedded, and Embodied Interaction (TEI '25)*, March 04, 2025. Association for Computing Machinery, New York, NY, USA, 1–12. https://doi.org/10.1145/3689050.3704956

- 602 [36] Ciarán T O'Neill, Connor M McCann, Cameron J Hohimer, Katia Bertoldi, and Conor J Walsh. Unfolding Textile-Based Pneumatic Actuators for Wearable Applications.
- [37] OtherLab. 2012. The Ant-Roach. Otherlab. Retrieved from https://www.otherlab.com/blog-posts/the-ant-roach-1
- [38] Jifei Ou, Mélina Skouras, Nikolaos Vlavianos, Felix Heibeck, Chin-Yi Cheng, Jannik Peters, and Hiroshi Ishii. 2016. aeroMorph Heat-sealing Inflatable Shape-change Materials for Interaction Design. In Proceedings of the 29th Annual Symposium on User Interface Software and Technology
 (UIST '16), Association for Computing Machinery, New York, NY, USA, 121–132. DOI:https://doi.org/10.1145/2984511.2984520
- 608 [39] Yeong Jae Park, Myung Gook Ko, Babar Jamil, Jiseong Shin, and Hugo Rodrigue. 2022. Simple and Scalable Soft Actuation Through Coupled Inflat-609 able Tubes. IEEE Access 10, (2022), 41993–42003. https://doi.org/10.1109/ACCESS.2022.3167964
- 610 [40] Lukas Rambold, Robert Kovacs, Conrad Lempert, Muhammad Abdullah, Helena Lendowski, Lukas Fritzsche, Martin Taraz, Patrick Baudisch. 2023.
 611 AirTied: Automatic Personal Fabrication of Truss Structures. In Proceedings of the 36th Annual ACM Symposium on User Interface Software and
 612 Technology (UIST '23), October 29-November 01, 2023, San Francisco, CA, USA. ACM, New York, NY, USA, 10 pages.
 613 DOI:https://doi.org/10.1145/3586183.3606820
- 614 [41] Marvin D. Rhodes. 1985. Deployable Controllable Geometry Truss Beam. Langley Research Center.

620

621

622 623

624

625

626

627

628

629

630

631

632

636

637

638

639

640

641

642

643

644

645

646

- 615 [42] Rivertex Technical Fabrics Group BV. EcosealTM 200. Retrieved from https://www.rivertex.com/en/product/200
- 616 [43] Daniela Rus and Michael T. Tolley. 2015. Design, fabrication and control of soft robots. *Nature* 521, 7553 (May 2015), 467–475. https://doi.org/10.1038/nature14543
- 618 [44] Ali Sadeghi, Alessio Mondini, and Barbara Mazzolai. 2017. Toward Self-Growing Soft Robots Inspired by Plant Roots and Based on Additive Manufacturing Technologies. Soft Robotics 4, 3 (September 2017), 211–223. DOI:https://doi.org/10.1089/soro.2016.0080
 - [45] Harpreet Sareen, Udayan Umapathi, Patrick Shin, Yasuaki Kakehi, Jifei Ou, Hiroshi Ishii, and Pattie Maes. 2017. Printflatables: Printing Human-Scale, Functional and Dynamic Inflatable Objects. In Proceedings of the 2017 CHI Conference on Human Factors in Computing Systems (CHI '17), Association for Computing Machinery, New York, NY, USA, 3669–3680. DOI:https://doi.org/10.1145/3025453.3025898
 - [46] Valkyrie Savage, Carlos Tejada, Mengyu Zhong, Raf Ramakers, Daniel Ashbrook, and Hyunyoung Kim. 2022. AirLogic: Embedding Pneumatic Computation and I/O in 3D Models to Fabricate Electronics-Free Interactive Objects. In Proceedings of the 35th Annual ACM Symposium on User Interface Software and Technology (UIST '22), Association for Computing Machinery, New York, NY, USA, 1–12. DOI:https://doi.org/10.1145/3526113.3545642
 - [47] Shan-Yuan Teng, Cheng-Lung Lin, Chi-huan Chiang, Tzu-Sheng Kuo, Liwei Chan, Da-Yuan Huang, and Bing-Yu Chen. 2019. TilePoP: Tile-type Pop-up Prop for Virtual Reality. In Proceedings of the 32nd Annual ACM Symposium on User Interface Software and Technology (UIST '19), October 17, 2019. Association for Computing Machinery, New York, NY, USA, 639–649. https://doi.org/10.1145/3332165.3347958
 - [48] Robert F. Shepherd, Filip Ilievski, Wonjae Choi, Stephen A. Morin, Adam A. Stokes, Aaron D. Mazzeo, Xin Chen, Michael Wang, and George M. Whitesides. 2011. Multigait soft robot. Proceedings of the National Academy of Sciences 108, 51 (December 2011), 20400–20403. https://doi.org/10.1073/pnas.1116564108
- 633 [49] Ali Shtarbanov. 2021. FlowIO Development Platform the Pneumatic "Raspberry Pi" for Soft Robotics. In Extended Abstracts of the 2021 CHI Conference on Human Factors in Computing Systems (CHI EA '21), May 08, 2021. Association for Computing Machinery, New York, NY, USA, 1–6.
 635 https://doi.org/10.1145/3411763.3451513
 - [50] Ryo Suzuki, Ryosuke Nakayama, Dan Liu, Yasuaki Kakehi, Mark D. Gross, and Daniel Leithinger. 2020. LiftTiles: Constructive Building Blocks for Prototyping Room-scale Shape-changing Interfaces. In Proceedings of the Fourteenth International Conference on Tangible, Embedded, and Embodied Interaction (TEI '20), Association for Computing Machinery, New York, NY, USA, 143–151. DOI:https://doi.org/10.1145/3374920.3374941
 - [51] Alexander Spinos, Devin Carroll, Terry Kientz, and Mark Yim. 2017. Variable topology truss: Design and analysis. In 2017 IEEE/RSJ International Conference on Intelligent Robots and Systems (IROS), September 2017. IEEE, Vancouver, BC, 2717–2722. https://doi.org/10.1109/IROS.2017.8206098
 - [52] Saiganesh Swaminathan, Michael Rivera, Runchang Kang, Zheng Luo, Kadri Bugra Ozutemiz, and Scott E. Hudson. 2019. Input, Output and Construction Methods for Custom Fabrication of Room-Scale Deployable Pneumatic Structures. In Proceedings of the ACM on Interactive, Mobile, Wearable and Ubiquitous Technologies, 62:1-62:17. DOI:https://doi.org/10.1145/3328933
 - [53] M. Takeichi, K. Suzumori, G. Endo, and H. Nabae. 2017. Development of Giacometti Arm with Balloon Body. IEEE Robotics and Automation Letters 2, 2 (April 2017), 951–957. DOI:https://doi.org/10.1109/LRA.2017.2655111
- 647 [54] Nathan S. Usevitch, Zachary M. Hammond, Mac Schwager, Allison M. Okamura, Elliot W. Hawkes, and Sean Follmer. 2020. An untethered isoperimetric soft robot. *Sci Robot* 5, 40 (March 2020), eaaz0492. https://doi.org/10.1126/scirobotics.aaz0492
- 649 [55] Velcro IP Holdings LLC. Hook and Loop Tape, Double Sided VELCRO® Brand Fasteners. velcro.com. Retrieved from https://www.velcro.com/busi-650 ness/products/self-engaging-and-back-to-back/
- Fenelope Webb, Valentina Sumini, Amos Golan, and Hiroshi Ishii. 2019. Auto-Inflatables: Chemical Inflation for Pop-Up Fabrication. In Extended Abstracts of the 2019 CHI Conference on Human Factors in Computing Systems (CHI EA '19), May 02, 2019. Association for Computing Machinery, New York, NY, USA, 1–6. https://doi.org/10.1145/3290607.3312860
- [57] Michael Wehner, Ryan L. Truby, Daniel J. Fitzgerald, Bobak Mosadegh, George M. Whitesides, Jennifer A. Lewis, and Robert J. Wood. 2016. An integrated design and fabrication strategy for entirely soft, autonomous robots. *Nature* 536, 7617 (August 2016), 451–455.
 DOI:https://doi.org/10.1038/nature19100
- Yue Yang, Lei Ren, Chuang Chen, Bin Hu, Zhuoyi Zhang, Xinyan Li, Yanchen Shen, Kuangqi Zhu, Junzhe Ji, Yuyang Zhang, Yongbo Ni, Jiayi Wu,
 Qi Wang, Jiang Wu, Lingyun Sun, Ye Tao, and Guanyun Wang. 2024. SnapInflatables: Designing Inflatables with Snap-through Instability for
 Responsive Interaction. In Proceedings of the CHI Conference on Human Factors in Computing Systems (CHI '24), May 11, 2024. Association for Computing Machinery, New York, NY, USA, 1–15. https://doi.org/10.1145/3613904.3642933